JOURNAL OF CHEMICAL & ENGINEERING DATA

ARTICLE

pubs.acs.org/jced

Ion Association in Dilute Aqueous Magnesium Sulfate and Nickel Sulfate Solutions Under Hydrothermal Conditions by Flow Conductivity Measurements

Melerin Madekufamba and Peter R. Tremaine*

Department of Chemistry, University of Guelph, 50 Stone Road East, Guelph, Ontario, Canada, N1G 2W1

ABSTRACT: Electrical conductivities of very dilute aqueous solutions of magnesium sulfate and nickel sulfate ($\sim 10^{-3}$ mol·kg^{-1}) were measured at temperatures from (398.15 to 548.15) K and from (398.15 to 498.15) K, respectively, with an alternating current (AC) conductivity flow cell at a pressure of 18.62 MPa. The resulting conductivity data were modeled using the Fuoss−Hsia−Fernández−Prini (FHFP) conductance equations together with the appropriate activity coefficient expressions, to obtain equilibrium constants for the ion association reactions: $Mg^{2+}(aq) + SO_4^{2-}(aq) \rightleftharpoons MgSO_4^{\circ}(aq)$ and $Ni^{2+}(aq) + SO_4^{2-}(aq) \rightleftharpoons NiSO_4^{\circ}(aq)$. The equilibrium constants K_A for the two systems, which correspond to the formation of all types of ion pairs (solvent−solvent-separated, solvent-separated, and contact ion pairs), agree remarkably well with results calculated from solubility measurements at much higher concentrations. The results were described by the temperature-dependent equilibrium constant model to a precision of ± 0.03 in log K_A.

1. INTRODUCTION

The effect of temperature and pressure on the association of 2:2 electrolytes has been a topic of active investigation since the pioneering studies of Noyes and his co-workers at the Carnegie Institute more than 100 years ago.[1,2] A wide variety of studies using conductance,[1−4] potentiometry,[5] solubility,[6−8] calorimetry,[9] densimetry,[10] and osmotic pressure methods[11,12] have been used to derive thermochemical models for these systems. These have been complemented by techniques such as ultrasonic absorption,[13] Raman spectroscopy,[14−16] UV−visible spectroscopy,[17] and dielectric relaxation spectroscopy (DRS),[18,19] which have been proven to be powerful tools for distinguishing between different types of ion pairs, the so-called "solvent−solvent-separated", "solvent-separated", and "contact" ion pairs. Most of these methods are limited to temperatures near ambient conditions, either because of experimental constraints or because many of the metal sulfate salts display inverse solubility relationships at elevated temperatures which limits the use of instruments that require solution concentrations greater than ~0.05 mol·kg^{-1}.[2,6,8,11−16]

Magnesium sulfate is a constituent of many systems including, but not limited to, biological systems, seawater, natural brines, geothermal fluids, and industrial processes. The ability of aqueous $MgSO_4$ to form strong ion pairs was identified early in the history of solution chemistry, and its role as a model system for exploring the nature of ion-pair formation explains why this system has been widely investigated under ambient conditions. Although a number of careful experimental studies have been carried out on $MgSO_4$ under hydrothermal conditions,[2,3,5,6,8,11,12,14] most of these were limited to temperatures below 473 K by the inverse solubility of the salt.

Nickel sulfate solutions are used at temperatures up to 453 K in recently developed hydrometallurgical processes to recover nickel from lateritic ores. Aqueous nickel sulfate can also be formed as a corrosion product of stainless steel and inconel in the boiler circuits of thermal and nuclear electrical power plants. While several studies of ion association in $NiSO_4$ solutions under hydrothermal conditions have been reported in the literature,[5,7,8,12] these are also restricted to temperatures below about 473 K, by solubility constraints.

Flow AC conductance is an attractive tool for extending the temperature range of association studies on metal sulfates because the method is very sensitive to ion pairing and can be employed to yield quantitative formation constants at concentrations as low as 10^{-5} mol·kg^{-1}.[4] Although conductivity techniques for measuring ion association at high temperatures and pressure have been available for many years, instruments sensitive enough to make measurements for dilute solutions under such extreme conditions have only recently been developed.[20−23] This work reports conductivity measurements for a series of dilute solutions of magnesium sulfate up to 548.15 K and nickel sulfate up to 498.15 K at a constant applied pressure of ~20 MPa. The data were used to obtain temperature-dependent equilibrium constants for the ion association reactions, under conditions where "solvent−solvent-separated" and "solvent-separated" ion pairs are the dominant associated species.

2. EXPERIMENTAL SECTION

2.1. Chemicals and Materials. Stock solutions of $MgSO_4$(aq) and $NiSO_4$(aq) were prepared by mass from ReagentPlus grade (> 99.5 %) anhydrous $MgSO_4$(s) and ReagentPlus grade (99.995 %) $NiSO_4.6H_2O$(s), both from Sigma Aldrich, without

Special Issue: John M. Prausnitz Festschrift

Received: July 9, 2010
Accepted: January 3, 2011
Published: January 28, 2011

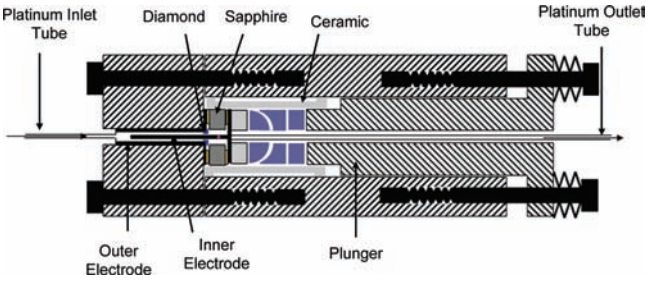

Figure 1. Schematic diagram of the AC conductance high-pressure flow cell.

further purification. The water content in $MgSO_4(s)$ was determined to be 0.17 % by drying at 573 K to a constant mass over a period of several days. Similarly, the exact hydration number of the nickel sulfate hexahydrate, $NiSO_4 \cdot nH_2O$, was determined to be n = (5.996 ± 0.005) by drying the green crystals of the commercial product at 573 K for ~16 h until the yellow anhydrous $NiSO_4$ had reached a constant mass. KCl solutions, for use in calibrating the conductance cell, were prepared by mass from ACS reagent grade KCl (Sigma Aldrich ReagentPlus, 99.0 %) that was dried for 48 h at 573 K before use. Milli-Q deionized water with a resistivity of 18 MΩ·cm was used to prepare all of the solutions. Dilutions to experimental concentrations were done by mass.

2.2. AC Conductance Measurements. The high-temperature, high-pressure conductance flow cell used for this work was built at the University of Delaware by Hnedkovsky et al.,[22] with improvements on the original designs of Sharygin et al.,[21] and Zimmerman et al.,[20] to allow for operation with more corrosive solutions. A schematic diagram is shown in Figure 1. Briefly, the cell consists of a 60 cm long temperature-controlled platinum inlet tube (1.0 mm inner diameter (i.d.); 1.6 mm outer diameter (o.d.)) that leads into a platinized cup (4.6 mm i.d.; 5.6 mm o.d.), which serves as the outer electrode for the cell. The inner electrode is a platinum rod (1.6 mm o.d.), electrodeposited with platinum black, and is a direct extension of the platinum tube which carries the exiting solution away from the cell. The entire electrode assembly is contained in a titanium cell body, which sits in a large air oven capable of controlling temperature to ± 0.15 K over several hours. The electrical insulation between the two electrodes is provided by a sapphire disk and ceramic spacer. The complex impedance of the cell containing aqueous solutions was measured at the following set of frequencies [(100, 300, 500, 1000, 2000, 4000, 6000, 8000, and 10 000) Hz] using a programmable automatic RCL meter (Fluke model PM6304), to obtain both the real and imaginary components of the impedance spectrum at each frequency.

The pressure seal inside the cell was maintained by compressing annealed thin gold disks which sit between the sapphire insulator and a titanium end-cap, using a system of bolts and Belleville washers. The pressure of the flowing solutions was controlled with the high-performance liquid chromatography (HPLC) injection system, described below. The temperature was measured with a platinum resistance standard (Hart Scientific, model 5612) to an accuracy of ± 0.02 K, and pressure was measured with a digital pressure transducer (Paroscientific Inc. model 760-6K) to a precision of ± 0.01 MPa. A detailed description of the cell was given by Hnedkovsky et al.[22] It has been used at temperatures as high as 673 K at 28 MPa, with ionic strengths as low as 10^{-5} mol·kg^{-1}.[22]

The injection system for the conductance equipment was very similar to that reported by Méndez de Leo and Wood.[24] Briefly, the sample to be injected was contained in a HPLC injection loop (3.2 mm o.d., passivated stainless steel tubing from Restek), with a capacity of 50 mL. Dual piston pumps, series 1500 from Lab Alliance, were used to inject deionized water into the high-pressure flow system, from a large reservoir whose temperature was maintained at 353 K to minimize the concentration of dissolved carbon dioxide. One pump, which was controlled through a computer with Hewlett-Packard VEE version 6.1 software, was used to pressurize the sample loop, or it bypassed the cell and flowed directly to waste while a sample was being injected into the cell. The second pump, which was always turned on, was used to inject a continuous flow of water through the cell, then to push the sample into the conductance cell. Two computer-controlled valves determined whether solution from the injection loop or water from the reservoir flowed through the conductance cell. Experiments were conducted at a flow rate of 0.5 mL·min^{-1}.

A set of glass bottles, equipped with KIMAX GL-45 gastight tops, contained the solutions of $MgSO_4(aq)$, $NiSO_4(aq)$, and KCl(aq) and deionized water, for injection into the high-pressure flow system. These were kept under a positive helium pressure for the duration of the experimental runs. A peristaltic pump, under computer-control and connected to a 14 port valve (VICI CHEMINERT 08U 056OL), was used to fill the loop in sequence with solutions taken from individual bottles.

2.3. Methods. AC impedance data were collected for a series of concentrations of $MgSO_4(aq)$ and $NiSO_4(aq)$ using the automatic injection system described above. Each sample injection was followed by a long injection of deionized water from the main reservoir, typically (50 to 80) mL, to rinse the equipment until the cell conductance had returned to its baseline value. This was followed by a measurement of the impedance of deionized water from a helium-blanketed bottle to provide impedance data so that we could correct the solution impedances for impurities. The injection cycle was then repeated with another solution. A typical set of measurements on eight samples at one temperature took about 40 h, of which data collection for each solution took about 2 h was followed by an additional (2.5 to 3) h to rinse the cell.

The result of these measurements was a series of values for the real and imaginary impedance, $Z_{Re}(\omega)$ and $Z_{Im}(\omega)$, as a function of frequency, ω:

$$Z(\omega) = Z_{Re}(\omega) - jZ_{Im}(\omega) \quad (1)$$

where Z is the complex impedance and Z_{Re} and Z_{Im} are the real and imaginary components of the impedance. The experimental conductivity of the solution (κ_s^{obs}) was calculated from R_s, the resistance of the solution at infinite frequency as estimated from an AC equivalent circuit model discussed below.

$$\kappa_s = k_c/R_s \quad (2)$$

The cell constant k_c was determined before each set of runs by measuring the conductivity for a series of six KCl standard solutions [(10^{-4} to 10^{-3}) mol·kg^{-1}] at 298.15 K and 18.62 MPa at the same frequency settings as the test solutions, using equations given by Barthel et al. for KCl(aq).[25] The average value of the cell constant used for the entire data sets for both $MgSO_4(aq)$ and $NiSO_4(aq)$ was found to be k_c = (0.06327 ± 0.00098) cm^{-1}. The cell constant k_c was assumed to be independent of temperature, as was confirmed by previous workers.[20−23]

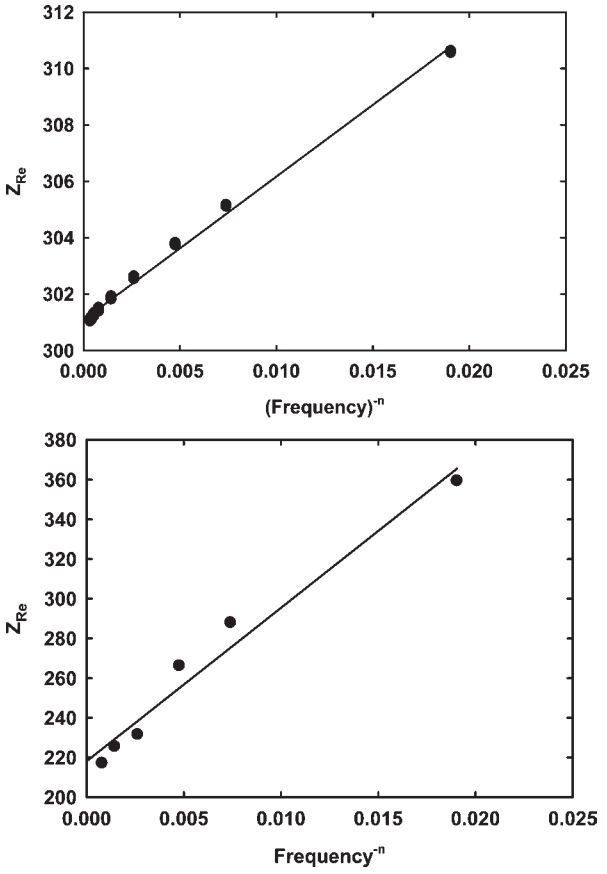

Figure 2. Frequency dependency of the real component of the impedance, Z_{Re} vs ω^{-n}, for (a) $MgSO_4$(aq) at $m = 3.0102 \cdot 10^{-4}$ mol·kg^{-1}, T = 398.15 K, and P = 19.18 MPa; and (b) $NiSO_4$(aq) at $m = 5.8672 \cdot 10^{-4}$ mol·kg^{-1}, T = 398.15 K, and P = 19.18 MPa. n = 0.86.

2.4. Impedance Data Treatment. The extrapolation of our impedance data to obtain the solution resistance at infinite frequency was done by two methods. The first used the equivalent circuit model described by Hnedkosky et al.[22] The model takes into account the following contributions to the measured impedance data: the solution resistance (R_s), the charge transfer resistance (R_{ct}), the capacitance of the conductance cell (C_{cell}), the double layer capacitance (C_d), and the Warburg impedance ($Z_{Warburg}(\omega)$). The Warburg impedance is represented by a frequency-dependent resistance $R(\omega)_{Warburg}$ and capacitance $C_{Warburg}(\omega)$ in series. Nonlinear least-squares fits using the full model showed that the charge transfer resistance and double layer capacitance terms were not statistically significant. To address this issue, we made use of the observation that the Warburg impedance for the water calibration runs was small and could be neglected. Fits to the data for pure water yielded a value for C_{cell} and approximate values for C_d and R_{ct}. These were then used as fixed parameters in fitting the model to the data for the aqueous solutions, which had much larger Warburg contributions. The resulting three-parameter fits agreed with the impedance data at all frequencies to within the estimated experimental uncertainty and yielded values for the solution resistance, R_s. The relative magnitude of the charge-transfer resistance used in the fits, R_{ct}/R_s, was less than 1 %. Our second method made use of the findings by Hnedkovsky et al.,[22] that very similar results to those from the equivalent circuit treatment can be obtained by extrapolating the function $Z_{Re} = R_s + a(\omega)^{-n}$ to infinite frequency, using the exponential term n as a fitting factor. The best fits, obtained using n = 0.86 for all our runs, yielded values for R_s that agreed with method 1 to within one percent. Typical plots of Z_{Re} versus $(\omega)^{-n}$ are shown in Figure 2.

3. RESULTS

Molar conductivities were calculated from the observed experimental conductivities κ_s^{obs}, after correcting for the specific conductivity of the impurities in the solvent, using the expression:

$$\Lambda = (\kappa_s^{obs} - \kappa_{solvent}^{obs})/c \quad (3)$$

Here, c is the concentration of the solution in mol·L^{-1}, $\kappa_{solvent}^{obs}$ is the experimental specific conductivity of deionized water, and κ_s^{obs} is the conductivity of the electrolyte solution, as calculated by the method of Hnedkosky et al.[22] Solution concentrations for these dilute solutions were calculated from molalities using the densities from Hill's equation of state for water.[26] The molar conductivity results for $MgSO_4$ and $NiSO_4$ are tabulated in Tables 1 and 2, respectively, together with the measured values of the experimental specific conductivity of water.

The molar conductivity data were treated with the Fuoss−Hsia−Fernández−Prini (FHFP) conductivity model.[27,28] The FHFP equation describes the ionic strength dependence of specific conductivity. The model for fully dissociated electrolytes, which is restricted to symmetric electrolytes (i.e., 1:1, 2:2, or 3:3 electrolytes), at ionic strengths below 0.01 mol·L^{-1}, is expressed by the following set of equations.

$$\Lambda = \Lambda^\circ - S(c)^{1/2} + Ec\ln(c) + J_1 c - J_2(c)^{3/2} \quad (4)$$

$$S = \alpha^*\Lambda^\circ + \beta^* \quad (5)$$

$$\alpha^* = \frac{82.046 \cdot 10^4 z^2}{(\varepsilon T)^{3/2}} \quad (6)$$

$$\beta^* = \frac{8.2487 z}{\eta(\varepsilon T)^{1/2}} \quad (7)$$

Here, $\Lambda^\circ = \lambda^\circ_{M^{2+}} + \lambda^\circ_{SO_4^{2-}}$ is the limiting ionic conductivity of the ionic species. The limiting slope S and the electrophoretic term E depend on the charge type of the electrolyte, ionic mobility, the magnitude of charge z on the ions, and the properties of the solvent (static dielectric constant, ε, and viscosity, η). The expressions for the J_1 and J_2 coefficients also depend on the minimum distance of closest approach of the free ions, as defined by the Debye−Hückel equation, and the level of approximation used in developing the theory. The expressions used in this work are specific for symmetric electrolytes.[27,28]

The effect of ionic association on molar conductivity can be represented by including the degree of dissociation, α, which represents the fraction of the stoichiometric metal and sulfate that exists as free ions. The metal−sulfate ion association reactions take the form:

$$\underset{\alpha c}{M^{2+}(aq)} + \underset{\alpha c}{SO_4^{2-}(aq)} \rightleftharpoons \underset{(1-\alpha)c}{MSO_4^{o}(aq)} \quad (8)$$

where c is the stoichiometric molar concentration. The corresponding association constant is represented by eq 9,

$$K_{c,A} = (1-\alpha)c^o/(\alpha^2\gamma_\pm^2 c) \quad (9)$$

dx.doi.org/10.1021/je100729t |J. Chem. Eng. Data 2011, 56, 889–898

Table 1. Experimental Molar Conductivities for $MgSO_4$(aq)

$m \cdot 10^5$ / mol·kg^{-1}	$c \cdot 10^5$ / mol·L^{-1}	Λ / S·cm^2·mol^{-1}
$T = (399.67 \pm 0.02)$ K; $P = (19.18 \pm 0.01)$ MPa; $\kappa^{obs}_{solvent} = 1.53203 \pm 0.00078$ (μS·cm^{-1})		
30.102	28.127	824.5
80.175	75.842	669.3
145.24	136.40	566.3
324.98	305.20	434.4
631.83	593.34	329.9
30.102	28.127	820.5
80.175	75.842	669.3
145.24	136.40	566.3
324.98	305.20	440.4
631.83	593.334	331.9
$T = (424.95 \pm 0.02)$ K; $P = (19.15 \pm 0.01)$ MPa; $\kappa^{obs}_{solvent} = 2.73244 \pm 0.00095$ (μS·cm^{-1})		
30.102	27.911	905.0
80.175	74.872	702.5
145.24	134.66	582.6
324.98	301.32	437.0
631.83	585.84	326.9
30.102	27.911	895.0
80.175	74.872	702.5
145.24	134.66	582.6
324.98	301.32	437.0
631.83	585.84	326.9
$T = (448.15 \pm 0.02)$ K; $P = (18.87 \pm 0.01)$ MPa; $\kappa^{obs}_{solvent} = 3.06714 \pm 0.00059$ (μS·cm^{-1})		
30.102	27.219	987.0
80.175	72.966	706.5
145.24	131.24	567.6
324.98	293.65	407.0
631.83	570.92	291.9
30.102	27.219	983.0
80.175	72.966	700.5
145.24	131.24	560.6
324.98	293.65	405.0
631.83	570.92	300.9
$T = (473.89 \pm 0.02)$ K; $P = (18.83 \pm 0.01)$ MPa; $\kappa^{obs}_{solvent} = 3.30714 \pm 0.00095$ (μS·cm^{-1})		
30.102	26.408	990.0
80.175	70.842	760.5
145.24	127.42	608.6
324.98	285.10	425.0
631.83	554.30	322.9
30.102	26.408	993.0
80.175	70.842	761.5
145.24	127.42	603.6
324.98	285.11	423.0
631.83	554.30	313.9
$T = (500.26 \pm 0.02)$ K; $P = (18.71 \pm 0.01)$ MPa; $\kappa^{obs}_{solvent} = 3.51123 \pm 0.00098$ (μS·cm^{-1})		
30.102	25.534	893.0
80.175	68.484	606.5
145.24	123.18	472.6
324.98	275.61	328.0
631.83	535.30	260.9
30.102	25.534	895.0
80.175	68.484	608.5
145.24	123.18	473.6
324.98	275.61	327.0
631.83	535.30	264.9
$T = (523.15 \pm 0.02)$ K; $P = (18.64 \pm 0.01)$ MPa; $\kappa^{obs}_{solvent} = 3.74216 \pm 0.00101$ (μS·cm^{-1})		
30.102	24.538	839.1
80.175	65.528	547.8
145.24	118.40	413.0
324.98	264.92	285.9
631.83	515.07	205.0
30.102	24.538	837.4
80.175	65.528	548.8
145.24	118.40	413.0
324.98	264.92	285.9
631.83	515.07	203.0
$T = (547.26 \pm 0.02)$ K; $P = (18.82 \pm 0.01)$ MPa; $\kappa^{obs}_{solvent} = 4.25819 \pm 0.0085$ (μS·cm^{-1})		
28.102	21.852	912.1
61.890	48.126	644.8
95.137	73.979	535.8
194.98	151.62	388.6
370.8	288.54	275.8
28.102	21.852	913.6
61.890	48.126	645.1
95.137	73.979	537.1
194.98	151.62	387.9
324.98	288.54	276.3

where c° is the hypothetical 1 mol·L^{-1} standard state. The activity coefficient is defined by the Debye−Hückel equation:

$$\log \gamma_{c,\pm} = -\frac{A_\gamma (\alpha c)^{1/2}}{1 + \frac{50.2916 z a (\alpha c)^{1/2}}{(\varepsilon T)^{1/2}}} \quad (10)$$

where the term a is the distance of closest approach of the free ions, and the other symbols have their usual meaning.[27,28] As others have done,[10,27,28] the activity coefficient of the ion pair, $MgSO_4^\circ$, was set to unity. By combining eqs 4 and 9, the FHFP model for partially associated symmetrical electrolytes then takes the form:

$$\Lambda = \Lambda^\circ - S(\alpha c)^{1/2} + E\alpha c \ln(\alpha c) + J_1 \alpha c - J_2 (\alpha c)^{3/2} - K_{c,A} \Lambda \gamma_\pm^{\,2} (\alpha c) \quad (11)$$

Equation 11 was used to derive ion association constants from the experimental molar conductance data in Table 1 in the

Table 2. Experimental Molar Conductivities for $NiSO_4$(aq)

$m \cdot 10^5$	$c \cdot 10^5$	Λ
mol·kg^{-1}	mol·L^{-1}	S·cm^2·mol^{-1}
$T = (398.63 \pm 0.02)$ K; $P = (19.12 \pm 0.01)$ MPa; $\kappa^{obs}_{solvent} = 1.8306 \pm 0.00068$ (μS·cm^{-1})		
26.798	25.418	842.8
58.672	55.644	721.6
89.083	84.486	647.3
110.450	104.75	607.9
179.263	170.01	519.2
307.832	291.95	424.9
555.983	527.29	330.3
$T = (424.21 \pm 0.02)$ K; $P = (18.98 \pm 0.01)$ MPa; $\kappa^{obs}_{solvent} = 2.143 \pm 0.0042$ (μS·cm^{-1})		
26.798	24.847	918.6
58.672	54.402	786.2
89.083	82.597	677.1
110.450	102.41	645.5
179.263	162.26	542.2
307.832	285.43	420.3
555.983	515.51	325.8
$T = (448.19 \pm 0.02)$ K; $P = (18.77 \pm 0.01)$ MPa; $\kappa^{obs}_{solvent} = 3.348 \pm 0.0038$ (μS·cm^{-1})		
26.798	24.214	945.6
58.672	53.016	764.2
89.083	80.495	653.1
110.450	99.803	603.1
179.263	161.98	497.8
307.832	278.16	384.9
555.983	502.38	294.4
$T = (474.05 \pm 0.02)$ K; $P = (18.63 \pm 0.01)$ MPa; $\kappa^{obs}_{solvent} = 4.787 \pm 0.0021$ (μS·cm^{-1})		
26.798	23.512	985.2
58.672	51.474	761.2
89.083	78.152	674.4
110.450	96.898	604.4
179.263	157.27	493.8
307.832	271.06	389.1
555.983	487.76	288.9
$T = (498.65 \pm 0.02)$ K; $P = (19.13 \pm 0.01)$ MPa; $\kappa^{obs}_{solvent} = 6.513 \pm 0.0058$ (μS·cm^{-1})		
26.798	22.727	979.1
58.672	49.762	743.2
89.083	75.551	620.9
110.450	93.673	567.9
179.263	152.04	475.8
307.832	261.07	359.8
555.983	571.53	275.2

following manner. The parameters E, J_1, and J_2 were calculated using the theoretical form of the FHFP model.[28] In our first approach, model 1, the FHFP equation was fitted to the experimental data, using both the association constant K_A and

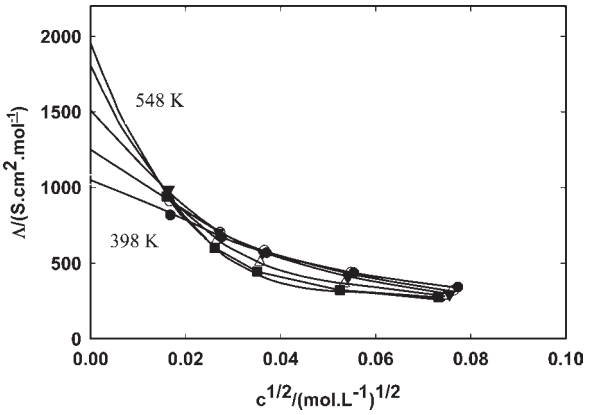

Figure 3. Molar conductivity of $MgSO_4$ as a function of concentration. The solid line is the FHFP equation, fitted using Λ° values from Marshall's reduced state relationships (model 2): ●, 398.15 K; ○, 423.15 K; ▼, 448.15 K; △, 473.15 K ; ■, 498.15 K.

the limiting molar conductivities of the ions, $\Lambda^0 = \lambda^0_{cation} + \lambda^0_{anion}$, as fitting parameters. In our second approach, model 2, the limiting molar conductivities were fixed to the values of Λ^0 predicted from the reduced state relationships reported by Marshall.[29] The properties of water (viscosity, η, and static dielectric constant, ε) were calculated from the equations of state reported by Archer and Wang.[30]

The FHFP equation requires values for the distance of closest approach of the free ions, a, and the corresponding reciprocal distance parameter, b, to calculate the relaxation terms J_1 and J_2. The two parameters are related to one another by the temperature and dielectric constant of the solvent, through the relationship:

$$b = \frac{16 \cdot 7099 \cdot 10^4 \cdot z^2}{a \cdot \varepsilon \cdot T} \qquad (12)$$

The data were best described by setting a value of the distance of closest approach for the ions $a = 6.3$ Å. This value is consistent with the work by Katayama,[31] which extended from (273 to 318) K and yielded values of $a = (6.3 \pm 0.2)$ Å above 303 K. This value for the distance of closest approach can be compared with values based on the ionic radii compiled by Marcus[32] which correspond to 2.95 Å and 3.00 Å for $MgSO_4$ and $NiSO_4$, respectively. Combining these values with the van der Waals diameter of water, 2.8 Å, suggests that the distance of closest approach corresponds to the inner-sphere solvent-separated ion pairs in which the metal and sulfate ions are separated by one water molecule, presumably the primary hydration sphere of the metal.

Figure 3 plots the experimental molar conductivity data for these dilute $MgSO_4$ solutions as a function of concentration and temperature, together with the fit of the FHFP model to the data at each temperature. As predicted by the Nernst−Einstein equation, the limiting molar conductivity of the free ions at infinite dilution, Λ°, increases sharply with temperature. This is balanced by an increase in the degree of association at elevated temperatures which causes the molar conductivity to decrease more strongly with concentration. The quality of the fit is illustrated in Figure 4, which plots the relative deviations of the fit from the experimental data, $(\Lambda - \Lambda^{Fit})/\Lambda$. The FHFP model represents the experimental data very well with calculated values that agree to within 3 % of the experimental data. Moreover, the deviations appear to be random, without systematic bias,

dx.doi.org/10.1021/je100729t |J. Chem. Eng. Data 2011, 56, 889–898

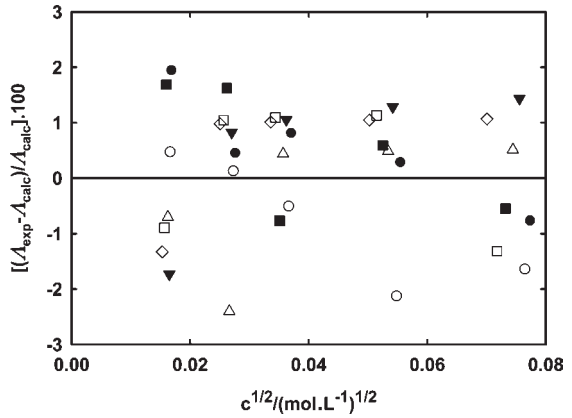

Figure 4. Relative deviations of measured molar conductivity for $MgSO_4$ aqueous solutions from the calculated values based on the FHFP conductivity model: ●, 398.15 K; ○, 423.15 K; ▼, 448.15 K; △, 473.15 K; ■, 498.15 K; □, 523.15 K; ♦, 548.15 K.

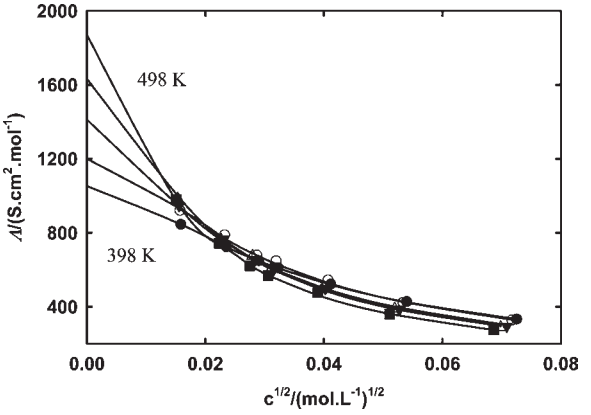

Figure 5. Molar conductivity of $NiSO_4$ as a function of concentration. The solid line is the FHFP equation, fitted using Λ° values from Marshall's reduced state relationships (model 2): ●, 398.15 K; ○, 423.15 K; ▼, 448.15 K; △, 473.15 K; ■, 498.15 K.

suggesting the FHFP is, in fact, the appropriate model to use for this system.[27] Figures 5 and 6 are similar plots of the experimental molar conductivity data for the $NiSO_4$ solutions, the fitted FHFP model, and its relative deviations from the experimental data. The temperature dependence of the limiting conductivity Λ° and the quality of the fit are similar to those reported above for the $MgSO_4$ solutions.

Values of the fitted ion-pair formation constants, K_A, and limiting molar conductivities, Λ°, are tabulated in Table 3. The fitted values of Λ^0 from Model 1 agreed with those predicted from Marshall's correlation[29] to with ± 5 % below 448 K. At higher temperatures they are increasingly more positive (20 % at T = 547 K); however, the difference in the fitted values of K_A from the two models is less than 1 %. The discrepancies of the fitted and predicted values of limiting conductance are within the stated uncertainties of Marshall's correlation.

The relationship between the equilibrium constant on the hypothetical unit-molality scale, K_A, and that on the unit-molarity scales, $K_{c,A}$, is:

$$K_A = K_{c,A} \cdot \rho_w \qquad (13)$$

where ρ_w is the density of water. Values of the ion-pair formation constants, $K_{c,A}$, from the FHFP fits were converted to K_A using

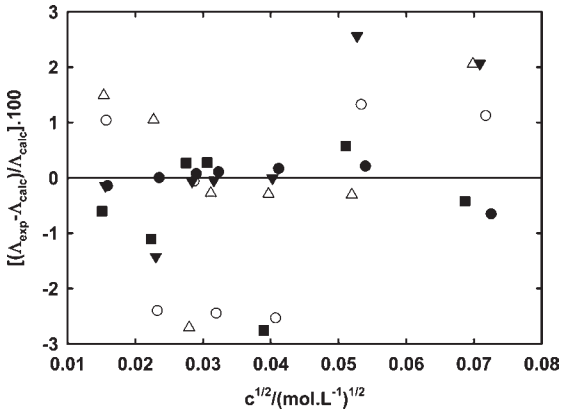

Figure 6. Relative deviations of measured molar conductivity for $NiSO_4$ aqueous solutions from the calculated values based on the FHFP conductivity model: ●, 398.15 K; ○, 423.15 K; ▼, 448.15 K; △, 473.15 K; ■, 498.15 K.

Table 3. Experimental Values for the Ion Association Constant (K_A) for the Systems $MgSO_4$(aq) and $NiSO_4$(aq), As Measured by Conductance

	model 1		model 2	
T/K	Λ°(Fit)	K_A	(Λ° ± 2 %)[a]	K_A
		$MgSO_4$ (aq)		
399.27	516.9 ± 0.9	1815 ± 7	524.3	1840 ± 19
424.95	650.0 ± 1.3	3048 ± 21	645.0	3124 ± 32
448.15	798.6 ± 0.8	5611 ± 7	755.2	5656 ± 9
473.89	949.3 ± 1.6	9482 ± 16	905.0	9874 ± 17
500.26	1031.5 ± 0.7	17606 ± 20	980.0	17433 ± 30
523.15	1195.4 ± 1.5	26454 ± 27	1070	26452 ± 48
547.26	1362.1 ± 0.6	40418 ± 31	1165	40423 ± 65
		$NiSO_4$ (aq)		
399.27	535.8 ± 0.9	1832 ± 7		
424.95	655.0 ± 0.6	3118 ± 2		
448.15	732.0 ± 0.7	5729 ± 7		
473.89	939.6 ± 1.6	10407 ± 22		
500.26	1054.6 ± 1.2	19111 ± 34		

[a] Calculated from Marshall's reduced state relationship.[8]

values for the density of water reported by Hill.[26] The tabulated uncertainties in Table 3 are the standard errors of the solution resistances obtained by fitting the models described in Section 2.4 to the frequency-dependent AC impedance data. In all cases these are less than 0.6 %. In addition to these statistical uncertainties, there is a systematic uncertainty due to the long-term drift in the cell constant, which is no more than 2 %. Finally, the hydrolysis of nickel, according to the reaction $Ni^{2+} + H_2O + SO_4^{2-} = NiOH^+ + HSO_4^{2-}$, competes with the formation of the ion pair $NiSO_4^0$. We estimate the maximum concentration of $NiOH^+$ to be no more than 6 % of the ion pair at the highest temperature and concentration studied. This contributed an additional systematic error of less than 3 % to the value reported for K_A at 500 K. The contribution of $NiOH^+$ at lower temperatures was negligible.

The results for K_A are plotted in Figures 7 and 8, along with values obtained by conductance methods from other workers.[31,33−35]

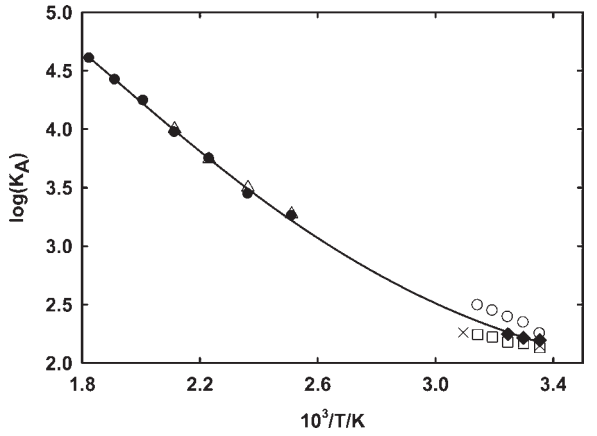

Figure 7. Temperature dependence of equilibrium constants $\log(K_A)$ for the $MgSO_4(aq)$ system: ●, this work; △, Marshall solubility;[6] □, Katayama conductance;[31] ○, Nair and Nancolas EMF;[36] ♦, Tomsic et al., conductance;[34] ×, Pethybridge and Taba;[33] —, eq 16.

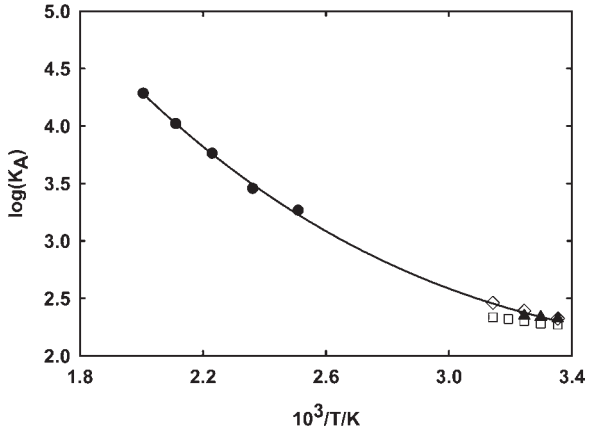

Figure 8. Temperature dependence of equilibrium constants $\log(K_A)$ for the $NiSO_4(aq)$ system: ●, this work; □, Katayama conductance;[31] ◊, Nair and Nancolas EMF;[37] ▲, Beštec-Rogač et al., conductance;[35] —, eq 17.

Values for $MgSO_4$ determined by Marshall[6] from solubility measurements are included in Figure 7 for comparison. The association constants for both systems show a rapid increase with temperature. The values for $NiSO_4$ are higher than those for $MgSO_4$ by about 0.13 units at 398 K and 0.04 units at 498 K in log K_A. The results are consistent with measurements near ambient conditions by Nair and Nancollas[36,37] using electromotive force (EMF) methods and with conductance measurements by Katayama,[31] Tomšič et al.,[34] and Beštec-Rogač et al.[35]

The temperature dependence of the association constants for $MgSO_4$ and $NiSO_4$ in Figures 7 and 8 could be represented well by thermodynamic models based on linear heat capacity functions in eq 15.

$$\ln K_{A,T} = \ln K_{A,T_r} - (\Delta H^{o}_{T_r}/R)\{(1/T) - 1/T_r)\} + (\Delta a/R)\{\ln(T/T_r) + (T/T_r) - 1\} + (\Delta b/2R)\{T + (T_r^2/T) - 2T_r\} \quad (14)$$

$$\Delta C^{o}_{p} = \Delta a + \Delta b T \quad (15)$$

Table 4. Parameters for Calculation of Equilibrium Constants (K_A) Based on Equations 13 and 14 for the Systems $MgSO_4(aq)$ and $NiSO_4(aq)$ at T_r = 298.15 K

		ΔH^{o}_{Tr}[a]	J·K^{-1}·mol^{-1}	J·K^{-2}·mol^{-1}
	log $K_{A,Tr}$	kJ·mol^{-1}	Δa	$\Delta b \cdot 10^3$
$MgSO_4(aq)$	2.194 ± 0.015	6.677 ± 0.050	20.481 ± 0.007	120.8 ± 1.8
$NiSO_4(aq)$	2.325 ± 0.035	4.610 ± 0.050	23.055 ± 0.313	−8.8 ± 0.2

[a] Refs 33 and 34.

Table 5. Standard Partial Molar Thermodynamic Quantities for the Equilibrium Reactions $Mg^{2+}(aq) + SO_4^{2-}(aq) \rightleftharpoons MgSO_4^{o}(aq)$ and $Ni^{2+}(aq) + SO_4^{2-}(aq) \rightleftharpoons NiSO_4^{o}(aq)$

T		ΔG^{o}	ΔH^{o}	ΔS^{o}	ΔC_p^{o}
K	log(K_A)	kJ·mol^{-1}	kJ·mol^{-1}	J·K^{-1}·mol^{-1}	J·K^{-1}·mol^{-1}
			$MgSO_4(aq)$		
298.15	1.966	−12.494	6.677[a]	64.30	56.50
323.15	2.170	−14.160	8.127	68.97	59.52
348.15	2.414	−15.941	9.653	73.52	62.54
373.15	2.679	−17.835	11.254	77.96	65.56
398.15	2.953	−19.838	12.931	82.30	68.58
423.15	3.225	−21.950	14.683	86.57	71.60
448.15	3.490	−24.166	16.511	90.77	74.62
473.15	3.744	−26.487	18.414	94.90	77.64
498.15	3.985	−28.911	20.393	98.97	80.66
523.15	4.211	−31.436	22.447	103.00	83.68
548.15	4.421	−34.060	24.576	106.97	86.70
573.15	4.791	−36.784	26.782	110.91	89.72
			$NiSO_4(aq)$		
298.15	2.081	−13.249	4.610[a]	59.90	20.43
323.15	2.293	−14.767	5.118	61.54	20.21
348.15	2.515	−16.325	5.621	63.03	19.99
373.15	2.746	−17.918	6.118	64.41	19.77
398.15	2.985	−19.545	6.609	65.69	19.55
423.15	3.232	−21.202	7.095	66.87	19.33
448.15	3.486	−22.888	7.576	67.98	19.11
473.15	3.746	−24.600	8.051	69.01	18.89
498.15	4.011	−26.337	8.520	69.97	18.67
523.15	4.283	−28.098	8.984	70.88	18.45

[a] Refs 33 and 34.

Here T_r = 298.15 K; $K_{A,Tr}$ is the value of K_A at 298.15 K; ΔH_{Tr}^{o} is the standard partial molar enthalpy of reaction at 298.15 K; R = 8.314510 J·K·mol^{-1} is the ideal gas constant; the parameters Δa and Δb were treated as fitting parameters.[38] Parameters for the models were obtained by least-squares fits to the data in Table 3, using the commercial software SigmaPlot Version 10. The fits were constrained to be consistent with the literature values for the standard thermodynamic properties at 298.15 K from the low temperature conductance measurements reported by Tomšič et al.[34] and Beštec-Rogač et al.[35] The fitted coefficients are tabulated in Table 4, along with their standard errors. Relative deviations in log K_A between the experimental data and fits by eqs 14 and 15 are plotted in Figure 9. Standard thermodynamic quantities for the association reactions calculated from eqs 14 and 15 are tabulated in Table 5.

dx.doi.org/10.1021/je100729t |J. Chem. Eng. Data 2011, 56, 889–898

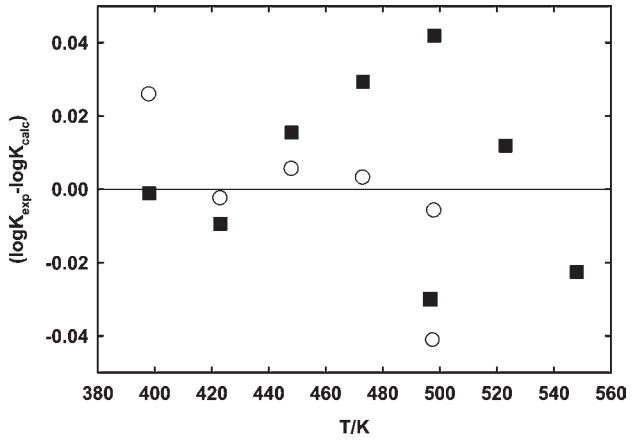

Figure 9. Relative deviations in log K_A between the equilibrium model, eq 14, and the experimental equilibrium constant data from the conductance experiments in this work: ■, $MgSO_4$(aq); ○, $NiSO_4$(aq).

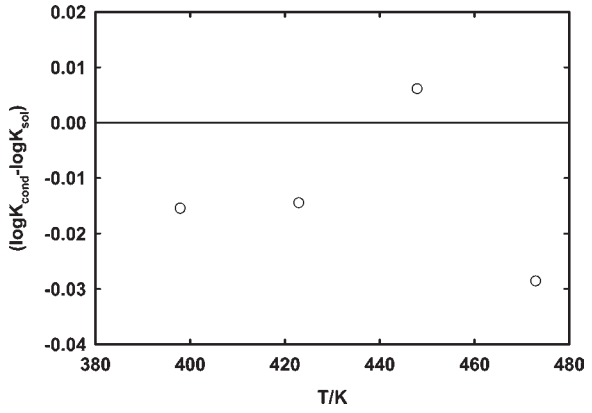

Figure 10. Relative deviations in log K_A between the equilibrium model from this work, eq 16, and equilibrium constant data calculated from experimental solubilities by Marshall.[6]

The fitted coefficients in Table 4 correspond to the following expressions for the equilibrium constants for ion-pair formation, for the $MgSO_4$(aq) system:

$$\log K_A = 144.91 + 55.941 \log(T/\mathrm{K}) + 4477.4/(T/\mathrm{K}) - 2.1995 \cdot 10^{-2} T/\mathrm{K} \quad (16)$$

and for the $NiSO_4$(aq) system:

$$\log K_A = 14.559 - 6.5658 \log(T/\mathrm{K}) - 217.62/(T/\mathrm{K}) + 1.5807 \cdot 10^{-2} T/\mathrm{K} \quad (17)$$

The major contribution to the standard error of ± 0.028 in log K_A, which corresponds to ± 6 % in K_A, arises from differences in the low temperature literature results used in the fit. The maximum deviation of the fits from our experimental values of K_A is ± 2 %.

4. DISCUSSION

The only reported experimental values for K_A of $MgSO_4$ above 350 K with which to compare our results are the pioneering conductance measurements of Noyes et al.[1,2] and the results reported by Marshall[6] from solubility measurements from (273.15 to 473.15) K, which are included in Figure 7. The deviations between our fitted expression for K_A, eq 15, and Marshall's values from solubility are plotted in Figure 10. The differences in log K_A are less than 1 %. This agreement is remarkable because Marshall's values were determined from solubility data at concentrations up to ~3 mol·kg^{-1}, using the simple extended Debye−Hückel expression:

$$\log \gamma_\pm = \frac{4AI^{1/2}}{1 + I^{1/2}} \quad (18)$$

Phutela and Pitzer,[39] Archer and Wood,[42] and Archer and Rard[11] reported more sophisticated thermodynamic models for aqueous $MgSO_4$, based on fitting the Pitzer ion-interaction model to the literature data available at the time. Two approaches were taken. In the first approach[11,19,35] the authors used only the activity coefficient formalism, with fitted expressions for the temperature-dependent pairwise and ternary interaction parameters in the Pitzer ion-interaction model. This approach does not yield an ion association constant for comparison with our results. The second approach, which was adopted by Archer and Wood,[42] used fitted equilibrium constants to represent the stepwise formation of associated ionic species, along with a simpler Pitzer ion-interaction model for the activity coefficients. Archer and Wood's treatment yielded statistically significant temperature-dependent equilibrium constants for three species, the 1:1 ion pair, $MgSO_4^\circ$; the 2:1 or 1:2 ion pair, $Mg_2SO_4^{2+}$ or $Mg(SO_4)_2^{2-}$ (which could not be distinguished); and the 3:3 species $Mg_3(SO_4)_3^\circ$. The association constants for all three species increased with increasing temperature. The formation constants of the 1:1 species reported by Archer and Rard[11] are listed in Table 6. Their value at 298.15 K, log K_{11} = 2.211 ± 0.025, agrees with the value in Table 4, log K_A = 2.194 ± 0.015, which was taken from Tomšič et al.[34] At higher temperatures, their fitted values for log K_{11} are much lower than our experimental values of log K_A.

More recently, Papangelakis and his co-workers[3] reported a thermodynamic model for the $MgSO_4$ system based on conductance measurements in the concentration range (0.01 to 0.4) mol·kg^{-1} and for $NiSO_4$ based on solubility data from the literature in the concentration range (0.1 to 1.5) mol·kg^{-1}.[40] The agreement is within 0.2 % at 523.15 K for the $MgSO_4$ and within 6 % for the $NiSO_4$ system.

Table 6. Association Constants for the $MgSO_4$ System Based on the Model by Archer and Rard[11]

T/K	log(K_{1-1})
298.15	2.211
323.15	2.309
348.15	2.440
373.15	2.596
398.15	2.768
423.15	2.952
448.15	3.144
473.15	3.341
498.15	3.541
523.15	3.742
548.15	3.944
573.15	4.145

It is important to identify the types of "ion-pairs" that are included in the association constants determined by AC conductance methods. Studies using ultrasonic absorption,[13] Raman spectroscopy,[14−16] and DRS[18,19] have shown that "solvent−solvent-separated", "solvent-separated", and "contact" ion pairs exist in equilibrium with one another. According to the simple scheme proposed by Eigen and Tamm,[13] these reactions can be characterized by stepwise equilibrium constants, written as:

$$M^{2+} + X^{2-} \overset{K_{SSIP}}{\rightleftharpoons} M^{2+}(H_2O)_2X^{2-} \overset{K_{SIP}}{\rightleftharpoons} M^{2+}(H_2O)X^{2-} \overset{K_{CIP}}{\rightleftharpoons} MX^{o} \quad (19)$$

Conductance measurements are sensitive to all types of ion pairs, so that the association constants reported here and elsewhere include the contribution of all three species:

$$K_A = K_{SSIP} + K_{SSIP}K_{SIP} + K_{SSIP}K_{SIP}K_{CIP} = \alpha/\{(1-\alpha)(m/m^o){\gamma_\pm}^2\} \quad (20)$$

Recent ab initio molecular dynamic (MD) calculations on aqueous $MgSO_4$[41] provide evidence for contact ion pairs and solvent-separated ion pairs, but there is no evidence for solvent−solvent separated ion pairs as distinct species. Thus, it appears that much of the contribution of "solvent−solvent-separated" ion pairs is due to nonspecific interactions that should be described by the theoretical electrophoretic and activity coefficient terms in the FHFP equation, rather than by including an equilibrium constant K_{SSIP} in eq 20. Hence, we believe that the fitted values of K_A from the FHFP model in Table 3 include, primarily, the contributions from K_{SIP} and K_{CIP}.

In the discussion above, we noted that the thermodynamic model by Archer and Wood[42] required terms for higher-order associated species, $Mg_2SO_4^{2+}$ or $Mg(SO_4)_2^{2-}$ and $Mg_3(SO_4)_3^{o}$. Dielectric relaxation studies from (278 to 340) K[18,19] and ab initio MD calculations[41] also provide evidence for the presence of 1:2 or 2:1 ion pairs at concentrations above about 0.1 mol·kg^{-1} and confirm that their stability increases with temperature. According to both the DRS studies[17] and the Archer−Wood model,[42] the triplet species should not be a significant factor at the concentrations (m < 0.01 mol·kg^{-1}) employed in our present study. The lower values of log K_{11} reported by Archer and Rard (Table 6), relative to our experimental values of log K_A in Table 4, suggest that all or part of the contributions of the solvent−solvent separated ion pairs and solvent-separated ion pairs are described by the Debye−Hückel and ion-interaction terms of the Pitzer model, so that their fitted values for log K_{11} are more closely associated with the contact ion-pair formation constant, log K_{CIP}.

We cannot account for the agreement of our results with the values log K_A obtained by Marshall[6] by fitting the very simple extended Debye−Hückel model, represented by eq 18, to his temperature-dependent solubility results. Although the agreement may be fortuitous, it appears that eq 18 can be used with eqs 16 and 17 to calculate the degree of association in $MgSO_4$ and $NiSO_4$ solutions from dilute solutions up to the solubility limit.

AUTHOR INFORMATION

Corresponding Author

*E-mail: mmadekuf@uoguelph.ca and tremaine@uoguelph.ca.

Funding Sources

Financial support from the Natural Sciences and Engineering Research Council (NSERC), Atomic Energy of Canada Ltd. and the University of Guelph is deeply appreciated.

ACKNOWLEDGMENT

We are grateful to Professor R. H. Wood at the University of Delaware for donating the conductance equipment to the University of Guelph and for his insightful advice. Professors Greg Zimmerman (Bloomsburg University) and Vladimiros Papangelakis (University of Toronto) provided much helpful advice and encouragement. Dr. Diego Raffa and Dr. Liliana Trevani, who transferred and set up the equipment at the University of Guelph, provided help and training in the use of the equipment and data-treatment software and many helpful discussions.

REFERENCES

(1) Noyes, A. A. The electrical conductivity of aqueous solutions. A series of experimental investigations executed by Noyes, A. A.; Coolidge, W. D.; Melcher, A. C.; Cooper, H. C.; Kato, Y.; Sosman, R. B.; Eastman, G. W.; Kanolt, C. W.; Böttger, W.; Carnegie Institute: Washington, DC, 1907; Publication No. 63.

(2) Noyes, A. A.; Melcher, A. C.; Cooper, H. C.; Eastman, G. W.; Kato, Y. The conductivity and ionization of salts, acids, and bases in aqueous solutions at high temperatures. *J. Am. Chem. Soc.* **1908**, *30*, 335–353.

(3) Huang, M.; Papangelakis, V. G. Electrical conductivity of concentrated $MgSO_4$-H_2SO_4 solutions up to 250 °C. *Ind. Eng. Chem. Res.* **2006**, *45*, 4757–4763.

(4) Corti, H. R.; Trevani, L. N.; Anderko, A. In *Aqueous Systems at Elevated Temperatures and Pressures: Physical Chemistry in Water, Steam and Aqueous Solutions*; Palmer, D. A., Fernandez-Prini, R., Harvey, A. H., Eds.; Elsevier Academic Press: Amsterdam, 2004; Chapter 10.

(5) Seneviratne, D. S.; Papangelakis, V. G.; Zhou, X. Y.; Lvov, S. N. Potentiometric pH measurements in acidic sulfate solutions at 250 °C relevant to pressure leaching. *Hydrometallurgy* **2003**, *68*, 131–139.

(6) Marshall, W. L. Aqueous Systems at High Temperature. XX. The dissociation constant and thermodynamic functions for magnesium sulphate to 200 °C. *J. Phys. Chem.* **1967**, *71*, 3584–3588.

(7) Marshall, W. L.; Gill, J. S; Slusher, R. Aqueous systems at high temperature-IV: Investigation on the system NiO-SO_3-H_2O and its D_2O analogue from 10^{-4} to 3 M SO_3 150 °C−450 °C. *J. Inorg. Nucl. Chem.* **1962**, *24*, 889–897.

(8) Marshall, W. L. Thermodynamic functions at saturation of several metal sulfates in aqueous sulfuric and deuterosulfuric acids at temperatures up to 350 °C. *J. Inorg. Nucl. Chem.* **1975**, *37*, 2155–2163.

(9) Woolley, E. M.; Hepler, L. G. Heat capacity of weak electrolytes and ion association reactions: method and application to aqueous solutions $MgSO_4$ and HIO_3 at 298 K. *Can. J. Chem.* **1977**, *55*, 158–163.

(10) Millero, F. J.; Masterton, W. L. Volume changes for the formation of magnesium sulphate ion pairs at various temperatures. *J. Phys. Chem.* **1974**, *78*, 1287–1294.

(11) Archer, D. G.; Rard, J. A. Isopiestic investigation of the osmotic and activity coefficient of aqueous $MgSO_4$ and the solubility of $MgSO_4 + H_2O$ at 298 K: Thermodynamic properties of the $MgSO_4 + H_2O$ system to 440 K. *J. Chem. Eng. Data* **1998**, *43*, 791–806.

(12) Holmes, H. F.; Mesmer, R. E. Isopiestic studies of aqueous solutions at elevated temperatures. VII. $MgSO_4$ and $NiSO_4$. *J. Chem. Thermodyn.* **1983**, *15*, 709–719.

(13) Eigen, M.; Tamm, K. Sound absorption in electrolytes as a consequence of chemical relaxation. I. Relaxation theory of stepwise dissociation. *Z. Elektrochem.* **1962**, *66*, 107–121.

(14) Rudolph, W. W.; Irmer, G.; Hefter, G. T. Raman spectroscopic investigation of speciation in $MgSO_4$(aq). *Phys. Chem. Chem. Phys.* **2003**, *5*, 5253–5261.

(15) Rudolph, W. W.; Brooker, M. H.; Tremaine, P. R. Raman spectroscopic investigations of aqueous $FeSO_4$ in neutral and acidic solutions from 25 to 303 °C inner and outer sphere complexes. *J. Solution Chem.* **1997**, *26*, 757–777.

(16) Rudolph, W. W.; Brooker, M. H.; Tremaine, P. R. Raman spectroscopy of aqueous $ZnSO_4$ Solutions under hydrothermal conditions: Solubility, hydrolysis, and sulfate ion pairing. *J. Solution Chem.* **1999**, *28*, 621–630.

(17) Mendez de Leo, L. P.; Bianchi, H. L.; Fernandez-Prini, R. Ion Pair Formation in Copper Sulfate Aqueous Solutions at High Temperatures. *J. Chem. Thermodyn.* **2005**, *37*, 499–511.

(18) Akilan, C.; Rohman, N.; Hefter, G.; Buchner, R. Temperature effects on ion association and hydration in $MgSO_4$ by dielectric spectroscopy. *ChemPhysChem* **2006**, *7*, 2319–2330.

(19) Chen, T.; Hefter, G.; Buchner, R. Ion association and hydration in aqueous solutions of nickel II and cobalt II sulfate. *J. Solution Chem.* **2005**, *34*, 1045–1066.

(20) Zimmerman, G. H.; Gruskiewicz, M. S.; Wood, R. H. New apparatus for conductance measurements at high temperatures: Conductance of aqueous solutions of LiCl, NaCl, NaBr and CsBr at 28 MPa and water densities from 700 to 260 kg m^{-3}. *J. Phys. Chem. B* **1995**, *99*, 11612–11625.

(21) Sharygin, A. V.; Wood, R. H.; Zimmerman, G. H.; Balashov, V. N. Multiple ion association versus redissociation in aqueous NaCl and KCl at high temperatures. *J. Phys. Chem. B* **2002**, *106*, 7121–7134.

(22) Hnedkovsky, L.; Wood, R. H.; Balashov, V. N. Electrical conductances of aqueous Na_2SO_4, H_2SO_4, and their mixtures: limiting conductances, dissociation constants, and speciation to 673 K and 28 MPa. *J. Phys. Chem. B* **2005**, *109*, 9034–9046.

(23) Ho, P. C.; Bianchi, H.; Palmer, D. A.; Wood, R. H. A new flow-through cell for precise conductance measurements of aqueous solutions to high temperatures and pressures. *J. Solution Chem.* **2000**, *29*, 217–235.

(24) Méndez De Leo, L. P.; Wood, R. H. Conductance Study of Association in Aqueous $CaCl_2$, $Ca(CH_3COO)_2$, and $Ca(CH_3COO)_2$•nCH_3COOH from 348 to 523 K at 10 MPa. *J. Phys. Chem. B* **2005**, *109*, 14243–14250.

(25) Barthel, J.; Feuerlein, F.; Neuder, R.; Wachter, R. Calibration of conductance cells at various temperatures. *J. Solution Chem.* **1980**, *9*, 209–219.

(26) Hill, P. G. A Unified fundamental equation for the thermodynamic properties of H_2O. *J. Phys. Chem. Ref. Data* **1990**, *19*, 1233–1274.

(27) Bianchi, H. L.; Dujovne, I.; Fernandez Prini, R. Comparison of electrolyte conductivity theories: performance of classical and new theories. *J. Solution Chem.* **1999**, *29*, 237–253.

(28) Fernández-Prini, R. Conductance and transfer numbers. In *Physical Chemistry of Organic Solvent Systems*; Covington, A. K., Dickson, T., Eds.; Plenum Press: London, 1973.

(29) Marshall, W. L. Reduced state relationship for limiting electrical conductances of aqueous ions over wide ranges of temperature and pressure. *J. Phys. Chem.* **1987**, *87*, 3639–3643.

(30) Archer, D. G.; Wang, P. The dielectric constant of water and Debye-Hückel limiting law slopes. *J. Phys. Chem. Ref. Data* **1990**, *19*, 371–411.

(31) Katayama, S. Conductometric determination of ion association constants for magnesium and nickel sulfates in aqueous solutions at various temperatures between 0 and 45 °C. *Bull. Chem. Soc. Jpn.* **1973**, *46*, 106–109.

(32) Marcus, Y. *Ion Solvation*; John Wiley and Sons Ltd.: London, 1985.

(33) Pethybridge, A. D.; Taba, S. S. Precise conductimetric studies on aqueous solutions of 2:2 electrolytes. Interpretation of new data in terms of the current theories of Pitts and Fuoss. *J. Chem. Soc., Faraday Trans. 1* **1980**, *6*, 274–284.

(34) Tomšič, M.; Beštec-Rogač, M.; Jamnik, A.; Neueder, R.; Barthel, J. Conductivity of magnesium sulfate in water from 5 to 35 °C from Infinite dilution to saturation. *J. Solution Chem.* **2002**, *31*, 19–31.

(35) Beštec-Rogač, M.; Babič, V.; Perger, T. M.; Neueder, R.; Barthel, J. Conductometric study of ion association of divalent symmetric electrolytes: I. $CoSO_4$, $NiSO_4$, $CuSO_4$ and $ZnSO_4$ in water. *J. Mol. Liq.* **2005**, *118*, 111–118.

(36) Nair, V. K. S.; Nancollas, G. H. Thermodynamics of ion association. IV. Magnesium and zinc sulphate. *J. Chem. Soc.* **1958**, 3706–3710.

(37) Nair, V. K. S.; Nancollas, G. H. Thermodynamics of ion association. VI. Some transition-metal sulphates. *J. Chem. Soc.* **1959**, 3934–3939.

(38) Anderson, G. M.; Crerar, D. A.; *Thermodynamics in Geochemistry: The Equilibrium Model*; Oxford University Press: New York, 1993.

(39) Phutela, R. C.; Pitzer, K. S. Heat capacity and other thermodynamic properties of aqueous magnesium sulphate to 473 K. *J. Phys. Chem.* **1986**, *90*, 895–901.

(40) Liu, H.; Papangelakis, V. G. Chemical modeling of high temperature aqueous processes. *Hydrometallurgy* **2005**, *79*, 48–61.

(41) Jahn, S.; Schmidt, C. Speciation in aqueous $MgSO_4$ fluids at high pressures and high temperatures from ab initio molecular dynamics and Raman spectroscopy. *J. Phys. Chem. B* **2010**, *114*, 15565–15572.

(42) Archer, D. G.; Wood, R. H. Chemical equilibrium model applied to magnesium sulphate solutions. *J. Solution Chem.* **1985**, *14*, 757–780.